LABELING HUMAN MOTION SEQUENCES USING GRAPHICAL MODELS

José I. Gómez
Dpt. Computer Science, University of Jaen, Campus Las Lagunillas, Jaen, Spain

Manuel J. Marín-Jiménez, Nicolas Pérez de la Blanca
Dpt. Computing Science and Artificial Intelligence, University of Granada, ETSI Informatica y Telecomunicacion Granada, Spain

Keywords: Data labeling, Pose estimation, Graphical models, Human motion.

Abstract: Graphical models have proved to be very efficient models for labeling image data. In particular, they have been used to label data samples from human body images. In this paper, the use of graphical models is studied for human-body landmark localization. Here a new algorithm based on the Branch&Bound methodology, improving the state of the art, is presented. The initialization stage is defined as a local optimum labeling of the sample data. An iterative improvement is given on the labeling space in order to reach new graphs with a lower cost than the current best one. Two branch prune strategies are suggested under a B&B approach in order to speed up the search: a) the use of heuristics; and b) the use of a node dominance criterion. Experimental results on human motion databases show that our proposed algorithm behaves better than the classical Dynamic Programming based approach.

1 INTRODUCTION

In this paper, graphical models based on Decomposable Triangulated Graphs (DTG) are used to approach the human-body landmark localization and tracking problems. Our approach is based on maximizing the likelihood of the probabilistic graphical model from a set of image measurements. Assuming that the object is present in the image, the localization problem relabels the sample data (image features) as part of the object or background. Different approaches have been proposed to label or match image data using graphical models (Gold and Rangarajan, 1996), (Grimson, 1990), (Haralick and Shapiro, 1992), (Rangarajan et al., 1997), (Ullman, 1996). Some of these techniques are very general in the sense that they are applied on any graphical model. However, these approaches are difficult to apply on data with a substantial amount of clutter. In (Caelli and Caetano, 2005), graphical models are favorably compared with traditional relaxation approaches. Figure 1 broadly shows the main steps of our approach to label new images from the learned DTG models. In the case of human motion labeling, the probability distribution defined by the learned graphical model, can be used as a constraint on the set of allowed graph configurations.

The new contributions of this paper are: *i*) we introduce a new graph labeling algorithm for the DTG class that improves the standard dynamic programming strategy; *ii*) we show how the DTG class is able to capture the human-body pose from different cameras and to identify the point of view.

1.1 Related Work

The DTG class (Amit and Kong, 1996) is introduced as a simpler graph class to register deformable patterns on static images. More recently, the same graphical model is used to label human body templates in tracking problems (Song et al., 2003). In both approaches, a Dynamic Programming algorithm (DP) was used as the search strategy to find the best labeling from a learned model (Fischler and Elschlager, 1973). In a DTG, each node represents a landmark of the object with an associated vector of measurements. Although dynamic programming is a very convenient technique to learn DTG models from data and also to label new sample data, this strategy presents three important drawbacks that are analyzed in depth in section 2.2. We propose a new algorithm that overcomes

I. Gómez J., J. Marín-Jiménez M. and Pérez de la Blanca N. (2009).
LABELING HUMAN MOTION SEQUENCES USING GRAPHICAL MODELS.
In *Proceedings of the Fourth International Conference on Computer Vision Theory and Applications*, pages 488-495
DOI: 10.5220/0001795704880495

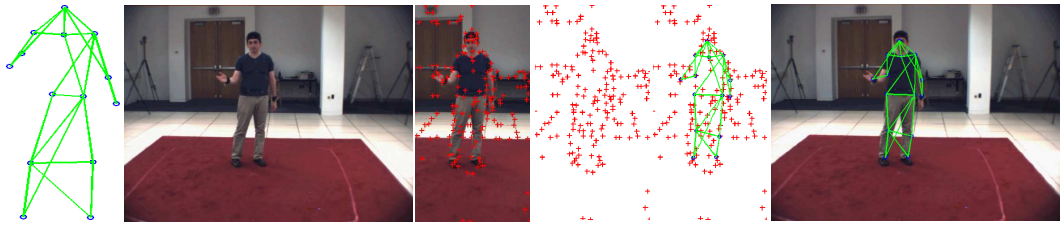

Figure 1: Aim of this work. (a) Learned model from data samples *'Gestures'*. (b) Input video frame. (c) Detected sample points around the person. (d) Input to labeling algorithm. (e) Best graph configuration found for input points and model *'Gestures'*. Blue circles represent the points selected by our labeling algorithm. (f) Superimposed graph on input video frame.

those drawbacks, based on a Branch&Bound (B& B) strategy.

The search for the best labeling is addressed by the minimum cost path on the tree of all possible labelings. However, the best labeling search problem is a NP-hard problem. Therefore, we approach the search by using a B& B strategy with an efficient pruning criterion on the labeling tree. This labeling space is explored using a first-in-depth strategy, delaying the final labeling assignment until a minimum cost solution has been found. Two branch prune strategies have been suggested under a B&B approach in order to speed up the search: a) the use of heuristics; and b) the use of a node dominance criterion (Fujino and Fujiwara, 1994), (Ibaraki, 1977), (Yu and Wah, 1988). Here we use a node dominance criterion because it best suits our problem. In order to obtain a worst case efficiency of $O(N^3)$, the same one using DP on this problem, we design our algorithm to get the best trade-off between search time and solution quality, according to the criterion established in (Hansen et al., 1997). In the experimental section 4, we show that our algorithm runs in $O(N^2)$ in most of our experiments.

Section 2 summarizes the probability model and discusses the labeling problem using a DTG model. Section 3 introduces our proposed labeling algorithm. Section 4 shows the experimental results using different human-body models. Section 5 presents our conclusions.

2 LABELING USING A DTG

2.1 The Probability Model

A Decomposed Triangulated Graph (DTG) is a triangle collection where there is a vertex elimination order so that the elimination of each node only affects one triangle (Figure 2). A greedy algorithm (Song et al., 2000), (Song et al., 2003) is proposed to estimate the probability model associated with a DTG from image data. Here we follow the notation introduced in (Song et al., 2003). Let $S = \{S_1, S_2, ..., S_M\}$ be a set of nodes, and let X_{Si}, $1 \leq i \leq M$ be the measure associated to each node. The probability model of a DTG describes the conditional dependences and independences of triplets of features associated with the triangles of the DTG. In this case, the probability density of the set of nodes is

$$P(X_{S_1}, X_{S_2}, ..., X_{S_M}) = P_{B_T C_T} \cdot \prod_{t=1}^{T} P_{A_t|B_t C_t} \qquad (1)$$

where $S = \{A_1, B_1, C_1, A_2, ..., A_T, B_T, C_T\}$; $(A_1, B_1, C_1), (A_2, B_2, C_2), ..., (A_T, B_T, C_T)$ are the triangles, and $(A_1, A_2, ..., A_T)$ is the vertex elimination order. Let $\chi = \{\overline{X}^1, \overline{X}^2, ..., \overline{X}^N\}$ be a set of samples where $\overline{X}^n = \{X^n_{S_1}, ..., X^n_{S_M}\}$, $1 \leq n \leq N$ represent the labeled data. We have to find the DTG G that maximizes the likelihood of the samples, $P(\chi|G)$, where

$$logP(\chi|G) \simeq -N \cdot h(X_{B_T}, X_{C_T}) - N \cdot \sum_{t=1}^{T} h(X_{A_t}|X_{B_t}, X_{C_t}) \qquad (2)$$

where $h(\cdot)$ is differential entropy or conditional differential entropy (Cover and Thomas, 1991). In other words, we want to find the best sequence $(A_1, B_1, C_1), (A_2, B_2, C_2), \cdots, (A_T, B_T, C_T)$ that minimizes $logP(\chi|G)$.

2.2 Searching for the Best Labeling

The search for the best labeling on a DTG using DP (Amit and Kong, 1996), (Song et al., 2000) has various drawbacks:

A) *Using DP the lowest cost node is always selected as the best candidate in the triangle building process.* The search process is carried out in the vertex elimination order fixed by the DTG. The label process starts by searching for the pair of sampled points with the least entropy and iterates adding new nodes. On each

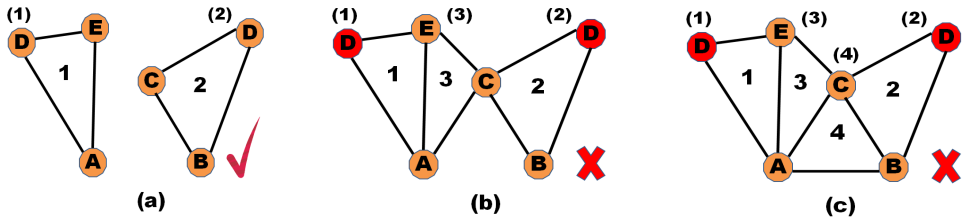

Figure 2: Example of DTG model on which the problem of vertex repetition is present. Between brackets the vertex elimination order for the model. (a) The first two triangles are obtained. We do not know yet whether these triangles are going to be in the same DTG; (b) The problem appears when triangle 3 links triangles 1 and 2 in the same DTG; (c) Wrong DTG obtained.

new iteration the sample point defining the least entropy triangle is labeled. Obviously, this early node assignment only allows to explore a very small subset of the labeling space skipping better optimum solutions.

B) *The same vertex (label node) can be associated with different sample points in the labeling process.* In Figure 2 we show a simple example of a DTG with six vertexes. Let us assume an image with n candidate points to be labeled as part of the model, where $n \geq 6$. Let us apply a labeling process using DP (Song et al., 2000), Figure 2 (a) shows two triangles built in the first step of the process. It is important to remark that in the building process of both triangles the label (D) has been used. Figure 2 (b) shows the time in which the DP algorithm decides to join both triangles. Only at this time it is possible to detect the problem. This imposes a high cost in time since we must go backwards and forwards in the labeling process in order to solve this problem (2 (c)).

C) *The DP efficiency lower bound is $T \cdot O(N^3)$ on DTG* (Amit and Kong, 1996), with N being the number of sample points and T being the number of triangles. Nevertheless, the DP solution is not the best possible one for this computational efficiency. In Section (4) we show that for most of our experiments it is possible to improve the DP labeling to $O(N^2)$. In addition, on more complex types of graph the lower bound of DP efficiency decreases linearly with the size of the greatest clique shown in the graph. This makes its use on complex graphs very inefficient.

3 ALGORITHM FEP

3.1 General Description

In this section we propose a new algorithm that overcomes the three drawbacks stated above. Let us assume a DTG model with T triangles and let triangle number T be the base triangle of the model. The triangle number 1 is then associated to the first vertex in the elimination order of the model. In order to define a cost for each base edge on each triangle and for each full triangle, the entropy measure associated to the vertexes in each case is used. In other words, for each triangle t with $1 \leq t \leq T$, $\Psi_t(X_{B_t}, X_{C_t}) = -h_t(X_{B_t}, X_{C_t})$ defines the cost of the base edge (X_{B_t}, X_{C_t}), and $\Psi_t(X_{A_t}, X_{B_t}, X_{C_t}) = -h_t(X_{A_t}, X_{B_t}, X_{C_t}) + h_t(X_{B_t}, X_{C_t})$ defines the cost of adding the vertex X_{A_t} to the edge (X_{B_t}, X_{C_t}) in order to build the triangle $(X_{A_t}, X_{B_t}, X_{C_t})$. Our goal is to find the labeling minimizing the value of $logP(\chi|G)$ as given by equation.2. On each iteration, we use Υ to denote the cost of the best DTG so far and Λ the cost of building the new DTG. $\Lambda < \Upsilon$ should of course be verified in order to proceed with the building process.

Let us assume N sample data (points), our approach is defined by two basic stages: a) to look for a first solution; and b) improve the current solution until efficiency reaches $O(N^3)$.

3.1.1 Looking for the First Solution

We start by building an ordered list of base edges, using all the possible pairs of nodes, by increasing value of their associated cost $\Psi_t(X_{B_t}, X_{C_t})$. Then we expand each edge associating to it the ordered list of candidate nodes also by increasing value of their cost. Iterating this process recursively and using a heuristic take-the-first on each expanding list, an initial best solution is obtained. The cost of this initial solution is the Υ initial value. The improving stage is defined from a prune strategy on the full labeling tree.

3.1.2 Iterative Improvement

For each list of candidate nodes to a triangle t we define a dynamic acceptance threshold, DAT, as a proportional value to the difference in entropy to the current best solution, $\Upsilon - \Lambda$, divided by the remaining number of triangles to fit $T - t + 1$,

$$DAT = \frac{\Upsilon - \Lambda}{T - t + 1} > 0 \qquad (3)$$

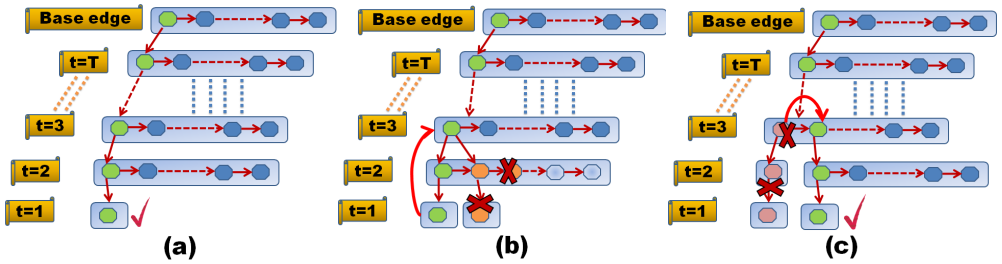

Figure 3: Algorithm FEP: (a) The initial best solution; (b) Searching for a better solution: if a worse DTG is found the branch is bounded; (c) When a better solution is reached, the best solution is updated. This process is repeated until no more candidate solutions left or $O(N^3)$ is reached.

This implies that as the iterative process progresses, the acceptance threshold for a new node decreases, thereby eliminating high cost candidates. Using the fitting cost and *DAT* value of the initial solution we initialize the best fitting cost Υ and the upper bound for the *DAT* value.

The iterative improvement progress from the initial solution as follows: *i*) we move two levels up in the labeling tree (Figure 3 (b)) from the leaf node of the initial solution; *ii*) from this new location we try to build a new solution branching down the second candidate of the associated node list (Figure 3(b)); *iii*) if the *DAT* value of the current node is lower than the upper bound for *DAT*, we move down first-in-depth adding the current node to the labeling; *iv*) we iterate again on the new node, using the same decision criteria until we reach a leaf node or the *DAT* value in the new node has a higher value than the *DAT* upper bound. On each leaf node we calculate $\Upsilon - \Lambda$, the fitting cost difference between the new solution and the best solution so far. If negative, we accept the new solution as the best current solution and we update the Λ and *DAT* upper bound value. Otherwise, we go up in the labeling tree and branch in breadth in order to evaluate the next node. If we reach an $O(N^3)$ efficiency during the search, we stop the process accepting as final solution the best current one.

3.2 Computational Complexity

We apply the technique proposed in (Hansen et al., 1997) to convert any heuristic search algorithm into an anytime algorithm offering a trade-off between search time and solution quality. In the fitting of a DTG using DP the computational complexity is always $O(T \cdot N^3)$ because the number of evaluated nodes is $NMAX_{DP} = T \cdot N \cdot (N-1) \cdot (N-2)$ (see (Amit and Kong, 1996), (Song et al., 2003)). Here we assume, without loss of generality, that the number of triangles of the DTG is $T > 2$, and the number of points on each frame is $N > 6$. In this context, $N^3 < NMAX_{DP}$. In FEP we set $NMAX_{DP}$ as the maximum number of nodes to evaluate, stopping the algorithm when this value is reached. We take into account the number of evaluated nodes in order to fix the actual efficiency achieved by FEP on each experiment. Our experiments show that a best case complexity of $\Omega(N^2)$ can be reached.

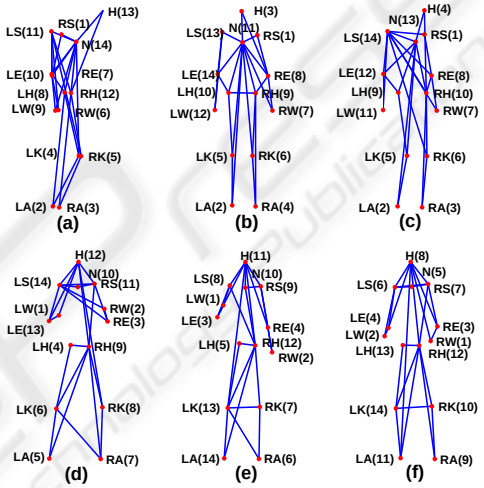

Figure 4: Caltech database (top row): Human DTG models for several points of view: (a) 0, (b) $\pi/2$, (c) $\pi/4$. HumanEva database (bottom row): frontal models for different actions: (d) *Boxing*, (e) *Gestures* and (f) *ThrowCatch*. In brackets, vertex elimination order for each DTG. In all cases $N = 14$ and $T = 12$.

4 EXPERIMENTS ON HUMAN LANDMARK LABELING

We have tested the performance of the FEP algorithm by carrying out different types of experiments. Firstly, we have learned human-body models using static and motion information in order to evaluate the fitted models. Secondly, we have tested the FEP per-

formance in order to discriminate among several models the best one representing a given set of sample points. In all the cases, we assume that the measure vector of the nodes follows a multivariate Gaussian distribution, which substantially simplifies the evaluation of the score measure given by equation (2) (see (Song et al., 2003)).

4.1 Database Description

We have used two different databases. The Caltech's Database (courtesy of C. Fanti), provides 3D information on a set of human-body landmarks in motion (Fanti et al., 2003). This database contains 3500 samples containing 3D information (position and velocity) of 14 fixed landmarks on a walking human body: head (H), neck (N), shoulders (LS,RS), elbows (LE,RE), wrists (LW,RW), hips (LH,RH), knees (LK,RK) and ankles (LA,RA). Experiments from different points of view, 0, $\pi/4$, $\pi/2$, $3\pi/4$ and π radians, have been conducted using the 3D information. In order to carry out experiments with more complex motions, we have also used some actions from the HumanEva database (Sigal and Black, 2006). The HumanEva database contains 4 actors performing a set of 6 actions each one in 3 separate trials. Here we focus on three of these actions: Box, Gesture and ThrowCatch. This database provides images from seven points of view: frontal view (camera C1), lateral views (C2 and C3), and 4 diagonal views (BW1, BW2, BW3 and BW4).

4.2 Labeling Experiments

The DTG models used in our experiments have been learned using the algorithm proposed in (Song et al., 2001). The labeling of a sample is considered correct if its cost is lower than the true cost assumed as known (only for the test samples). This criterion unfortunately does not guarantee that the fitted labeling is equal to the true one. The ambiguity defined by the relative location of the feet in a walking person seen from the side is impossible to solve by using this model, and this configuration will have an equal or lower cost than the true labeling. Also background points can be selected as part of the best labeling.

4.2.1 Caltech's Database

We have used 2500 image samples for learning the DTG models and 1000 for the labeling experiments. We learn two different types of models: a) static models, using only the projections of the 3D positions; b) motion models, using both the position and velocity projections. Some of the fitted models from this database are shown in Figure 4 (a)-(c). Once the models have been learned we use them to label the remaining 1000 samples.

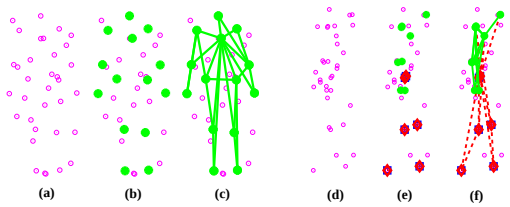

Figure 5: FEP working over two samples with 34 points (14+20): the first sample (a, b, c) shows a $\pi/2$ radians point of view where selected and expected points are coincident; the second sample (d, e, f) shows a 0 radians point of view where the points of both legs are exchanged; the remaining body points are fitted correctly. All the points in each sample are shown in (a) and (d); the points selected by FEP are shown in (b) and (e); finally, (c) and (f) show the fitted DTG. Green points: expected and selected labels are coincidents; red diamonds: selected labels are not coincident with expected labels; blue squares: expected labels that are not coincident with selected labels.

To compare the FEP and DP robustness under added noise, we run experiments with 14, 20 and 40 random added points over the original 14 points using the learned static and motion models. In Figure 6 (a) and (b), the results of both experiments are shown. It can be observed that in general FEP outperforms DP. Moreover, the percentage of samples with a labeling cost equal or lower than the original model is almost 100% for the FEP algorithm in all cases. Only for the samples in $3\pi/4$ angle do we have 97.8%. Moreover, in most of the experiments, FEP has $O(N^2)$ efficiency; only for angles $\pi/4$ and $3\pi/4$ does it reaches $O(N^3)$ in certain tests with added noisy points (see Figure 7). In figure 6 (c) and (d) a comparison on the timing efficiency of both techniques, FEP and DP, using the two models is shown. In all the cases, FEP outperforms DP.

It is not an easy task to establish a relationship between the set of graphs evaluated by FEP and DP respectively. The main difficulty is in the way the graph is built. DP starts from the first vertex according to vertex elimination order, while FEP starts from the base triangle, so that the first vertex in DP is the last added vertex in FEP. In order to assess the quality of the fitted graph given by DP and FEP, we run experiments on the Caltech's database counting the selected number of correct nodes by each algorithm. Figure 8 shows the obtained results using the motion model where both techniques provide equivalent performance. Results are very similar for the static model, so only motion model is shown in Figure 8.

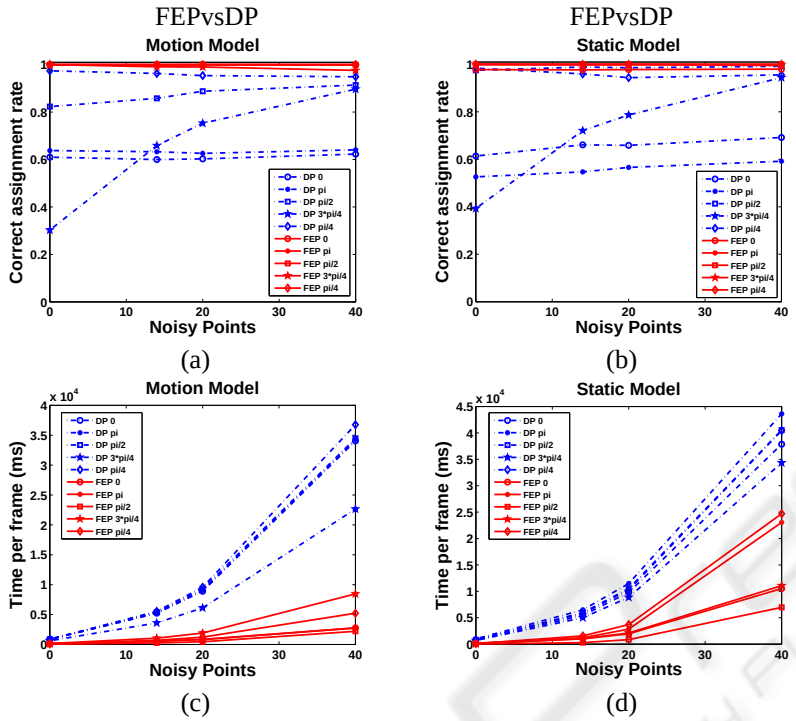

Figure 6: FEP versus DP: (a) and (b) performance measured in fitting cost, (c) and (d) timing per frame of FEP and DP respectively for two models, several angles and different number of noisy points added to the 14 labels used in our models (Figure 4).

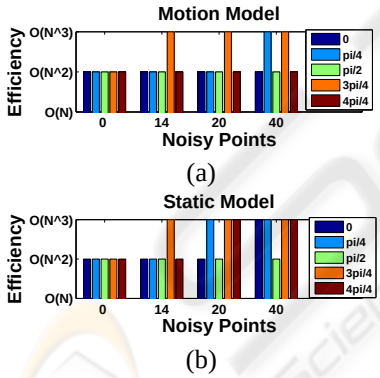

Figure 7: FEP computational complexity: (a) using motion information; (b) without using motion information. Measured on tests shown in Figure 6.

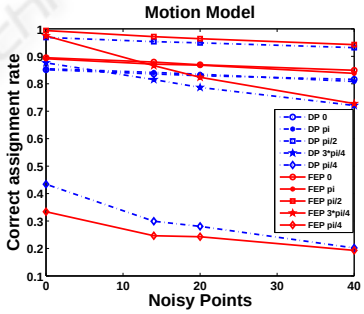

Figure 8: FEPvsDP: Ratio of correct labels using motion information.

4.2.2 HumanEva

For this database the same fourteen landmarks have been used. Between 6000 and 8000 image samples of the trial-3 of each action have been used for learning the DTG models. The only information used during the learning process is the projection of the true 3D coordinates of the selected landmark points on each actor. The 3D coordinates of the landmarks have been calculated from the information provided with the database. Models for the points of view associated to cameras C1, C2 and C3 have been learned. Figure 4(d)-(f) shows the learned frontal models for the camera C1. For the testing stage, about 1000 new image samples from trial-1, for each one of the actions and cameras, have been used. In this case the data samples have been generated projecting the full set of 3D landmark points provided by HumanEva (around 190) and selecting those projections inside a bounding box centered on each landmark projection. In average we obtained between 70 and 100 noisy points per sample, always including the fourteen landmarks of our model. Figure 9 (a) shows labeling examples on data

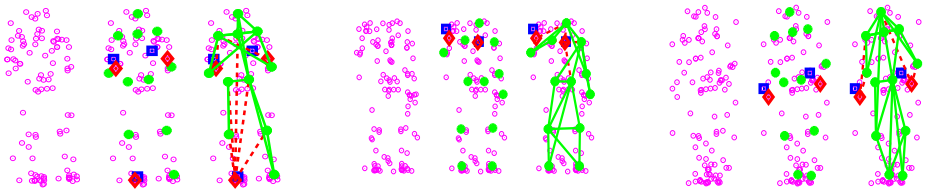

(a) (b) (c)

Figure 9: FEP working on HumanEva samples: (a) Box; (b) Gesture; (c) ThrowCatch. In all cases 14 landmarks and about 70-100 noisy points are used. See Figure 5 for color explanation.

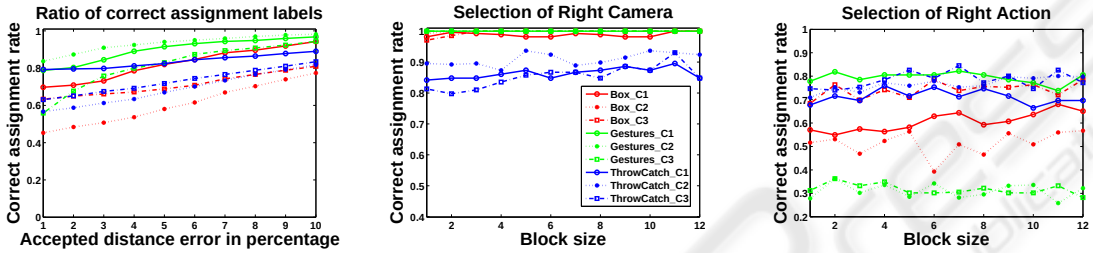

(a) (b) (c)

Figure 10: Results on HumanEva database: 9 different models combining actions and points of view are evaluated. In all cases the actor-1 was selected.(a) Ratio of correct assigned labels according to the distance to its ground-truth landmark.(b) Ratio of correct detected camera. Each sequence is evaluated with the 3 models associated to its own point of view against the remaining 6 models. Consecutive windows from 1 to 12 frames are classified on each decision. (c) Ratio of correct detected actions: the evaluation is performed using the 3 models associated to each action against the remaining 6 models.

from HumanEva using FEP.

Figure 10 (a) shows the FEP performance in selecting the ground-truth labels on each frame. In this experiment a labeled point is considered correct if its distance to the ground-truth landmark is less than a threshold in the range [1-10]% of the actor height. The best ratio is reached for the Gestures action.

4.3 Point of View and Action Discrimination

Regarding the application of DTG model in human-body tracking or motion capture applications, an important point is to select on each instant the best model according to the camera point of view. Experiments on HumanEva sequences have been conducted to evaluate the FEP capability on this task. Figure 10 (b) shows the FEP performance recognizing the right point of view model. It is remarkable that using a so simple scheme our results are very encouraging. In the worst case, the ratio of successful detection is greater than 80%. We have also conducted experiments on action recognition. Figure 10 (c) shows the capability of FEP to discriminate one action among several ones by choosing the model with the best fitting score. Obviously this problem is much more difficult that the previous one due to the high motion variability present on each action.In this experiment our aim is to recognize the action which is performed in blocks of different number of frames (ranging from 1 to 12 frames). We evaluate different DTG models on each frame in the target block. A majority vote scheme is finally used to assign an action class to each block. In this task, most of the test are above 70% of success and only for *Gestures* we have a score of 30%. This is well explained because the *Gesture* movements are so general that most of them are included as part of the other actions.

5 CONCLUSIONS

We have proposed a new algorithm (FEP), based on DTG models, which is able to find an optimal labeling on human motion data. Experiments have been carried out using two different databases: Caltech and HumanEva. It has been shown that on the Caltech‘s database the FEP algorithm is superior to the traditional DP algorithm both in terms of efficiency and quality of the found solution, in spite of its simplicity. The proposed approach could be generalized to deal with graphical models of higher complexity. This

point is the subject of forthcoming research.

ACKNOWLEDGEMENTS

This work was supported by the Spanish Ministry of Science and Innovation under projects TIN2005-01665 and Consolider Ingenio-2010 (MIPRCV).

REFERENCES

Amit, Y. and Kong, A. (1996). Graphical templates for model registration. *IEEE PAMI*, 18(3):225–236.

Caelli, T. and Caetano, T. S. (2005). Graphical models for graph matching: Approximate models and optimal algorithms. *Pattern Recognition Letters*, 26(3):339–346.

Cover, T. and Thomas, J. (1991). *Elements of Information Theory*. John Wiley and Sons.

Fanti, C., Polito, M., and Perona, P. (2003). An improved scheme for detection and labelling johanson displays. In *NIPS*.

Fischler, M. A. and Elschlager, R. A. (1973). The representation and matching of pictorial structures. *IEEE Trans. Comput.*, 22(1):67–92.

Fujino, T. and Fujiwara, H. (1994). A method of search space pruning based on search state dominance. *Journal of Circuits, Systems and Computers*, 25(4):1–12.

Gold, S. and Rangarajan, A. (1996). A graduated assignment algorithm for graph matching. *IEEE Trans. Pattern Anal. Mach. Intell.*, 18(4):377–388.

Grimson, W. E. L. (1990). *Object recognition by computer: the role of geometric constraints*. MIT Press, Cambridge, MA, USA.

Hansen, E. A., Zilberstein, S., and Danilchenko, V. A. (1997). Anytime heuristic search: First results. Technical Report UM-CS-1997-050.

Haralick, R. M. and Shapiro, L. G. (1992). *Computer and Robot Vision*. Addison-Wesley Longman Publishing Co., Inc., Boston, MA, USA.

Ibaraki, T. (1977). The power of dominance relations in branch-and-bound algorithms. *Journal of ACM*, 24(2):264–279.

Rangarajan, A., Chui, H., and Bookstein, F. L. (1997). The softassign procrustes matching algorithm. In *IPMI '97: Proceedings of the 15th International Conference on Information Processing in Medical Imaging*, pages 29–42, London, UK. Springer-Verlag.

Sigal, L. and Black, M. (2006). Humaneva: Synchronized video and motion capture dataset for evaluation of articulated human motion. Technical report, Brown University, Department of Computer Science.

Song, Y., Feng, X., and Perona, P. (2000). Towards detection of human motion. *IEEE Conference on Computer Vision and Pattern Recognition (CVPR)*, 1:810–817.

Song, Y., Goncalves, L., and Perona, P. (2001). Learning probabilistic structure for human motion detection. *IEEE Conference on Computer Vision and Pattern Recognition (CVPR)*, 2:771–777.

Song, Y., Goncalves, L., and Perona, P. (2003). Unsupervised learning of human motion. *IEEE Trans. Patt. Anal. and Mach. Intell.*, 25(7):1–14.

Ullman, S. (1996). *High-level Vision*. MIT Press.

Yu, C. and Wah, B. (1988). Learning dominance relations in combined search problems. *IEEE Transactions on Software Engineering*, 14(8):1155–1175.